**Molecular Cell, Volume *63***

## Supplemental Information

# Structure of a Cytoplasmic 11-Subunit RNA Exosome Complex

**Eva Kowalinski, Alexander Kögel, Judith Ebert, Peter Reichelt, Elisabeth Stegmann, Bianca Habermann, and Elena Conti**

**SUPPLEMENTAL MATERIAL**

**Supplemental Figure 1, related to Table 1**

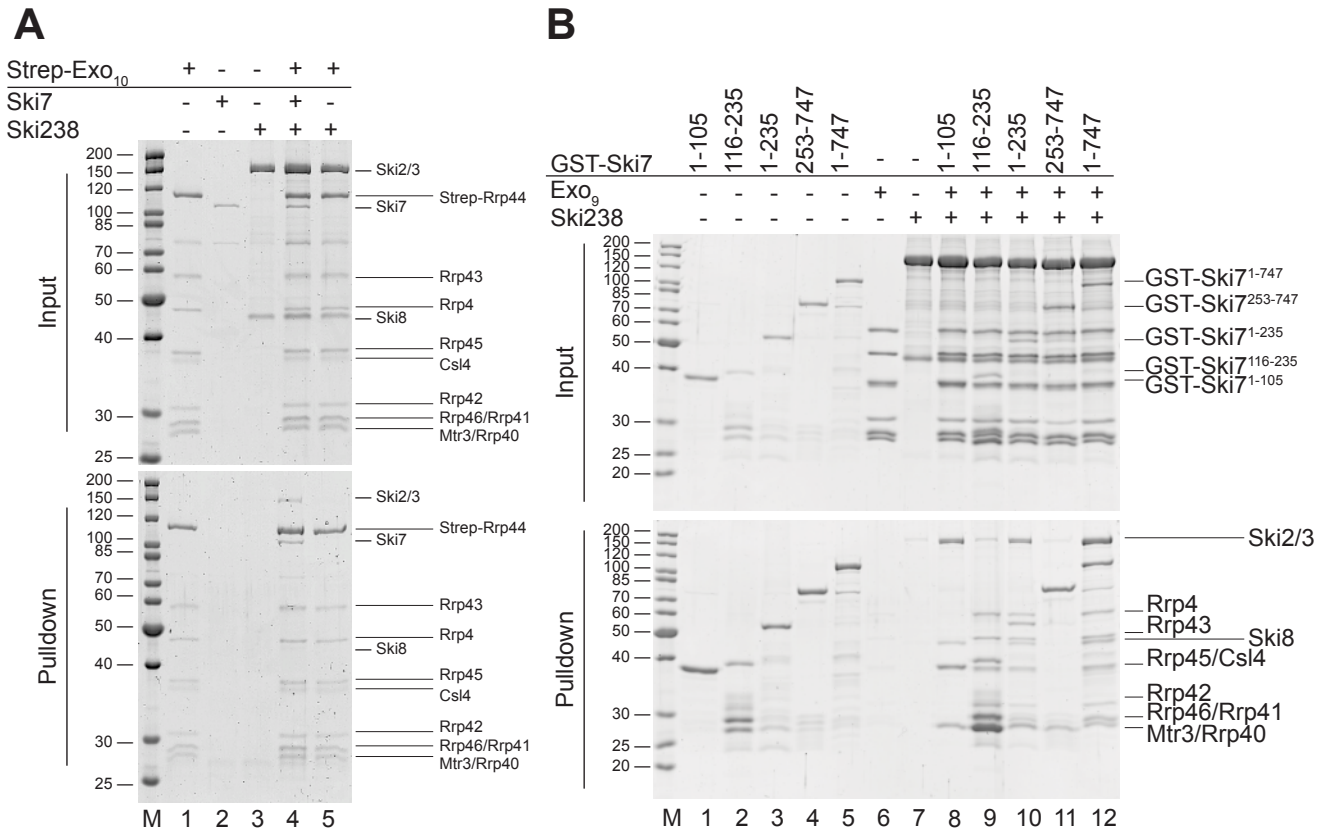


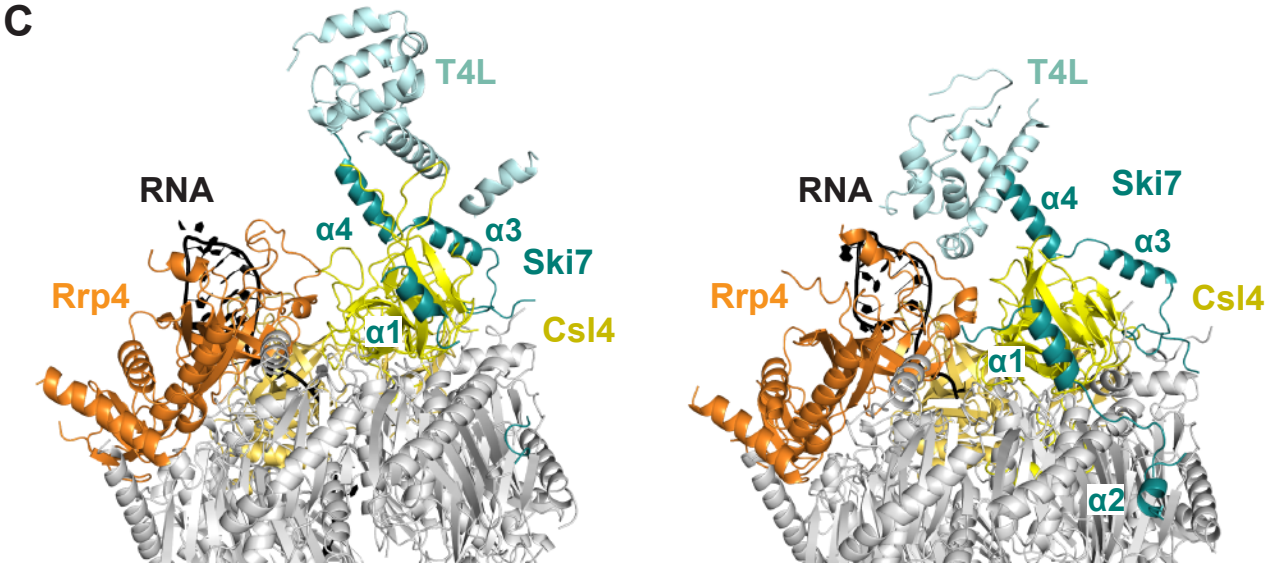

**Supplemental Figure 2, related to Figure 1**

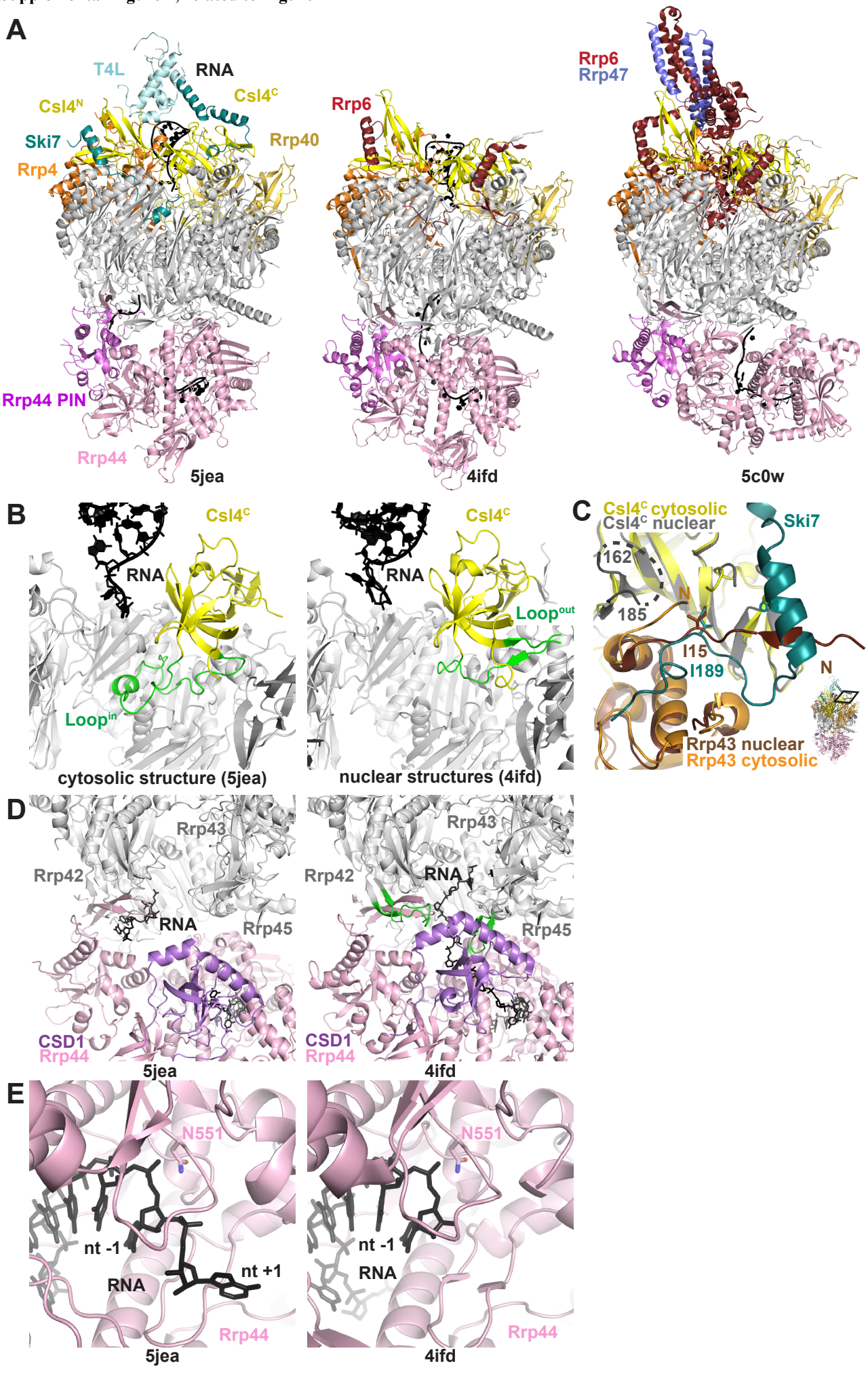

**Supplemental Figure 3, related to Figure 2**

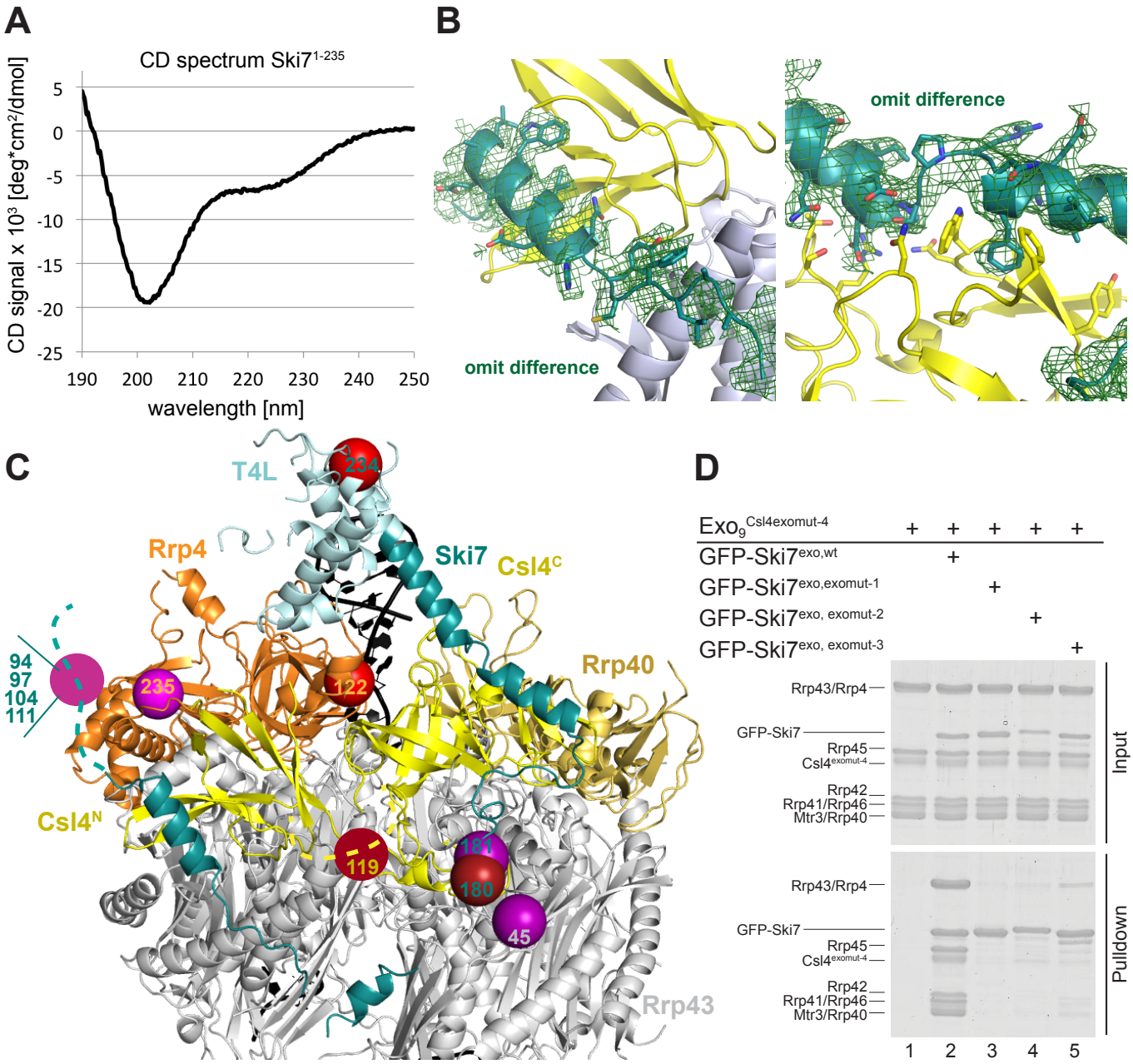

**Supplemental Figure 4, related to Figure 2**

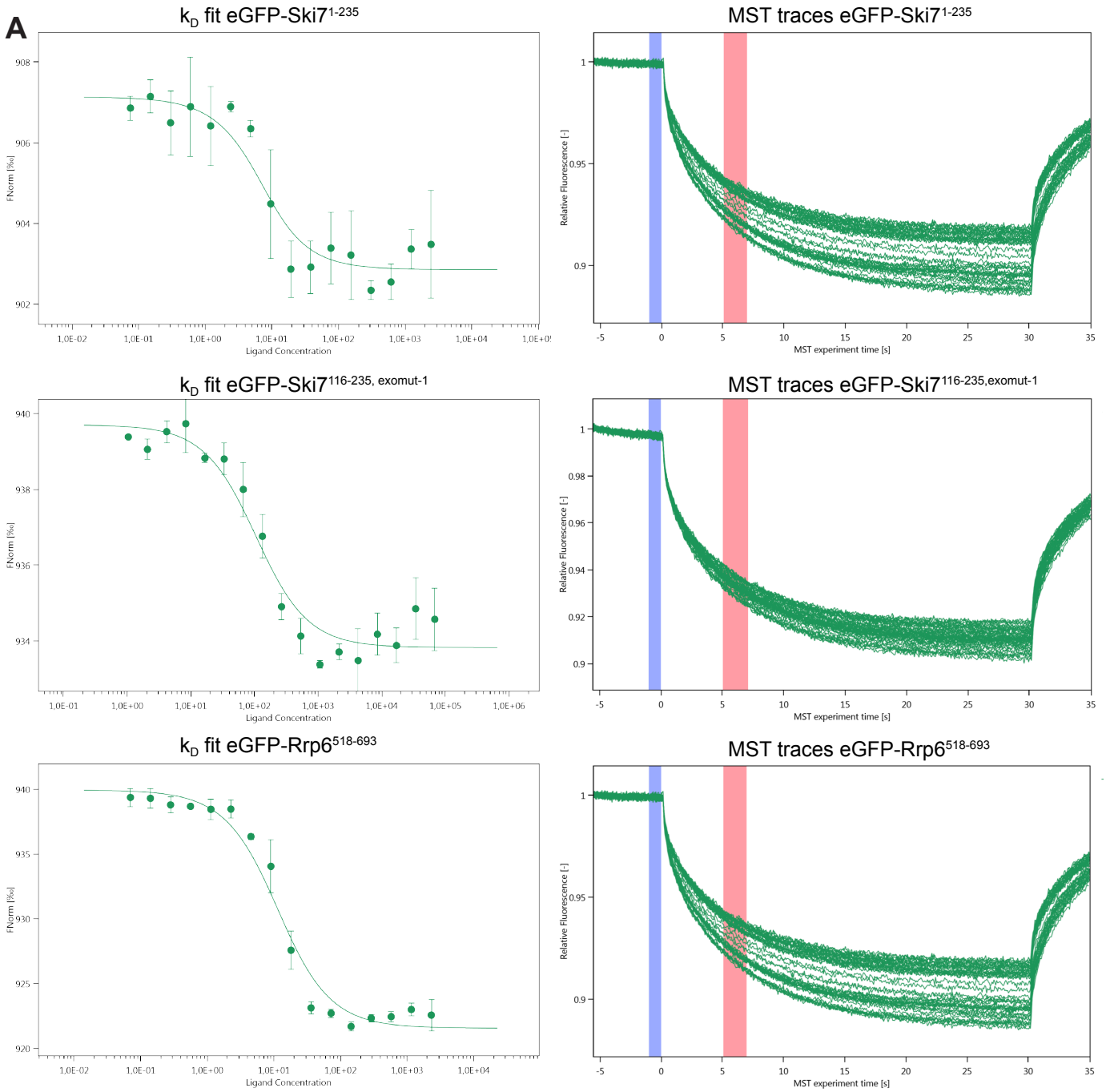


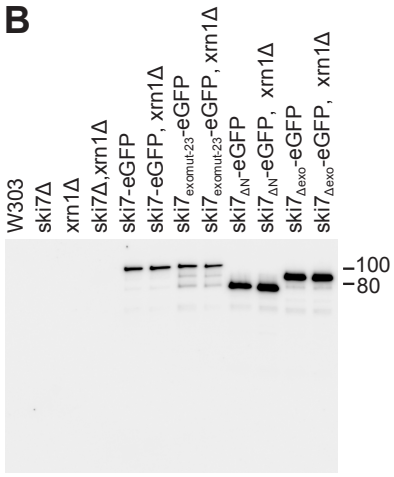

**Supplemental Figure 5, related to Figure 3**

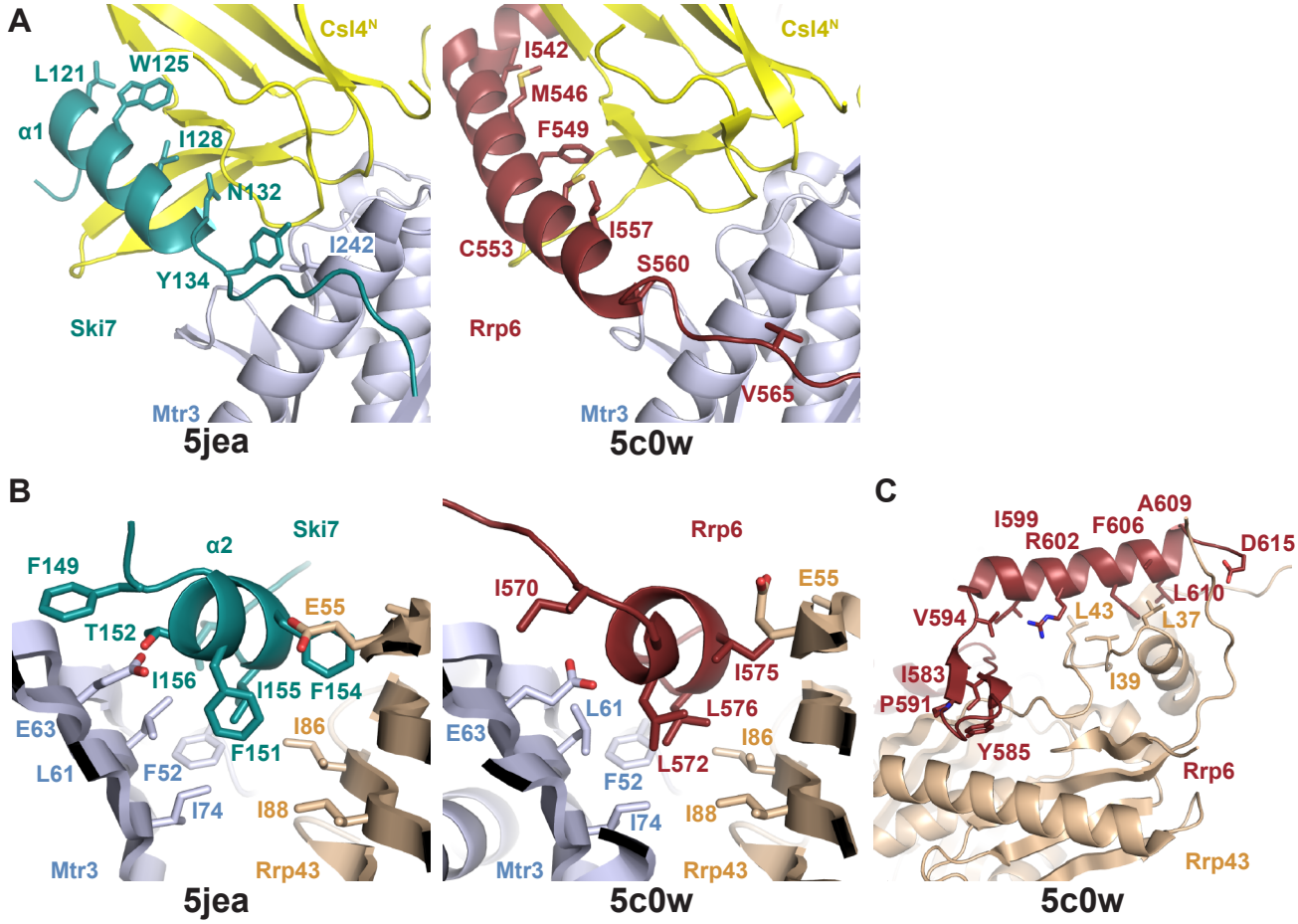


**Supplemental Table 1, related to Figure 2**

Yeast strains based on W303 *MATa/MATα {leu2-3,112 trp1-1 can1-100 ura3-1 ade2-1 his3-11,15, RAD5}*

| Label | ID | Relevant genotype |
|---|---|---|
| ski7Δ/SKI7 | scCLPR625 | W303 *MAT**a**/MATα, ski7Δ::klURA3/SKI7* |
| W303 | scCLPR272 | W303 *MATα , SKI7* |
| ski7Δ | scCLPR673 | W303 *MATα, ski7Δ::kanMX4, YCplac33 [XRN1, URA3]* |
| SKI7-EGFP | scCLPR676 | W303 *MAT**a**, ski7-EGFP::kanMX4, YCplac33 [XRN1, URA3]* |
| ski7$_{exomut-2-3}$ -EGFP | scCLPR678 | W303 *MAT**a**, ski7$_{exomut-2-3}$-EGFP::kanMX4, YCplac33 [XRN1, URA3]* |
| ski7$_{\Delta exo}$-EGFP | scCLPR680 | W303 *MATα, Δ116-235-ski7-EGFP::kanMX4, YCplac33 [XRN1, URA3]* |
| ski7$_{\Delta N}$-EGFP | scCLPR682 | W303 *MATα, Δ1-235-ski7-EGFP::kanMX4, YCplac33 [XRN1, URA3]* |
| xrn1Δ | scCLPR674 | W303 *MAT**a**, xrn1Δ::natNT2, YCplac33 [XRN1, URA3]* |
| ski7Δ/ xrn1Δ | scCLPR675 | W303 *MAT**a**, ski7Δ::kanMX4, xrn1Δ::natNT2, YCplac33 [XRN1, URA3]* |
| SKI7-EGFP, xrn1Δ | scCLPR677 | W303 *MAT**a**, ski7-EGFP::kanMX4 xrn1Δ::natNT2, YCplac33 [XRN1, URA3]* |
| ski7 $_{exomut-2-3}$ -EGFP, xrn1Δ | scCLPR679 | W303 *MAT**a**, ski7$_{exomut-2-3}$-EGFP::kanMX4 xrn1Δ::natNT2, YCplac33 [XRN1, URA3]* |
| ski7$_{\Delta exo}$-EGFP, xrn1Δ | scCLPR681 | W303 *MATα, Δ116-235-ski7-EGFP::kanMX4 xrn1Δ::natNT2, YCplac33 [XRN1, URA3]* |
| ski7$_{\Delta N}$-EGFP, xrn1Δ | scCLPR683 | W303 *MAT**a**, Δ1-235-ski7-EGFP::kanMX4 xrn1Δ::natNT2, YCplac33 [XRN1, URA3]* |
| mating strain | | |
| xrn1Δ | scCLPR476 | W303 *MAT**a**, xrn1Δ::natNT2, YCplac33 [XRN1, URA3]* |

**SUPPLEMENTAL FIGURE LEGENDS**

**FIGURE S1 (referring to Table 1)**
***In vitro* dissection of Ski7 interaction with the Ski-complex and the exosome.**
(A) Ski7 is necessary and sufficient for interaction of the exosome and the Ski complex. An SDS-PAGE of a pull down experiment of $Exo_{10}$ with Strep-tagged Rrp44 on Strep-tactin resin is shown. The Ski-exosome complex is only precipitated in the presence of Ski7 (lane 4) and not when Ski7 is absent (lane 5).
(B) Establishing minimal binding regions. In a GST pull down different GST-tagged Ski7 constructs were incubated with $Exo_9$ and GSH resin. $Ski7_{1\text{-}105}$ precipitates Ski-complex (lane 8), $Ski7_{116\text{-}235}$ precipitates $Exo_9$ (lane 9) and $Ski7_{1\text{-}235}$ and $Ski7_{1\text{-}747}$ precipitate both complexes (lanes 10 and 12). $Ski7_{235\text{-}747}$ (GTP binding domain) does not interact with either complex (lane 11).
(C) Optimization of the crystallization construct. The preliminary $Exo_{10}$ - $Ski7_{116\text{-}235}$T4L that yielded crystals diffracting to 4.2 Å on the left and the final $Exo_{10}$ - $Ski7_{116\text{-}225}$T4L that yielded crystals diffracting to 2.65 Å on the right.

**FIGURE S2 (referring to Figure 1)**
**Comparison of exosome structures.**
(A) Comparison of exosome complex structures. The $Exo_{10}$-Ski7 complex (5jea), $Exo_{10}$-Rrp6 complex (4ifd) and the $Exo_{10}$-Rrp6-Rrp47 (5c0w) complex are shown. Colours as in Figure 1B with Rrp6 in Red and Rrp47 in blue.
(B) Comparison of the Csl4 conformation in the cytosolic versus the nuclear exosome. 5jea and 4ifd are shown side by side. Representation and colors like Figure 1B, residues 158 to 200 of the described loop of Csl4 are shown in green.
(C) Ski7 is triggering the alternative Csl4 loop conformation. Superposition of the nuclear (4ifd) and the cytosolic exosome based on the C-terminal domain of Csl4. Nuclear Csl4 in grey, the outside position of the displaced loop is shown as dotted line, nuclear Rrp43 in chocolate. Colours of the cytosolic exosome like in Figure 1B. The nuclear conformation of the Rrp43 N-terminus is not compatible with the binding of Ski7, as both dock on the same surface of the exosome (with $Ile189^{Ski7}$ occupying the same position of $Ile15^{Rrp43}$). It is thus possible that the alternative conformation of the Rrp43 N-terminus upon Ski7 binding indirectly impinges on the position of the Csl4 loop and provokes a RNA-binding conformation inside the central channel instead of the solvent-exposed conformation as observed in the nuclear exosome.
(D) Mobility of the CSD1 domain of Rrp44. 5jea and 4ifd are shown side by side. Representation and colors like Figure 1C with the CSD1 domain of Rrp44 highlighted in purple. Loops of Rrp42 (residues 159-169) and Rrp43 (residues 250-270), that are disordered in 5jea are highlighted in green in the nuclear structure.
(E) The leaving position of the cleaved nucleotide in Rrp44. 5jea and 4ifd are shown side by side. Representation and colors like Figure 1E. The nuclear (4ifd) and the cytosolic exosome (5jea) were superposed based on the position of the RNB domain of Rrp44.

**FIGURE S3 (referring to Figure 2)**
**Additional biochemical data**
(A) Experimental data from a circular dichroism (CD) experiment. 10 µM $Ski7_{1\text{-}235}$ buffered in 20 mM NaPO4 pH 7.4, 50 mM NaF and subjected to a JASCO 810 Spectropolarimeter at 20 °C in a 1-mm path-length cuvette. The scan was taken from 250 to 190 nm in 0.1-nm increments and corrected by subtraction of the buffer spectrum. $Ski7_{1\text{-}235}$ is rather unstructured in solution.
(B) Example Fc-Fo map omitting Ski7 in the last step of refinement. Isomesh is shown in green at $\sigma = 1.5$ in a radius of 1.8 Å from the Ski7 chain. Views as in Figures 2B and 2E.
(C) Mapping mass-spec cross-linking data in the structure (Shi et al., 2015). Cross-linked residues are numbered and shown as spheres of the same color. Cross-linked residues in close-by loops (dotted lines) or beyond the boundaries of the crystallization constructs are shown as well, as colored circles or mapped in the corresponding residue in T4L, respectively. Cross-linked lysine residues: $87^{Ski7}$, $94^{Ski7}$, $104^{Ski7}$, $111^{Ski7}$ with $235^{Rrp4}$; $180^{Ski7}$ with $119^{Csl4}$ and $45^{Rrp43}$; $181^{Ski7}$ with $45^{Rrp43}$, $234^{Ski7}$ with $122^{Rrp4}$.
(D) Mutating a binding surface in patch 4 on Csl4 (Trp272Glu, Phe292Glu, Asn250Ala or $Csl4_{exomut\text{-}4}$) on the exosome only impairs the interaction with Ski7 in combination with one of the other binding patches mutated (lanes 3, 4 and 5). Protein co-precipitation in a GFP pull down assay is shown.

**FIGURE S4 (referring to Figure 2)**
**Additional biochemical data**
(A) Microscale thermophoresis traces (right) and $k_D$ fit curves (left) of constructs as annotated. $Exo_9$ was titrated. Cold (blue) and hot (red) regions that were used for analysis are marked in the traces. Experiments were conducted in triplicates and averaged before the curve fit as indicated by error bars.
(B) eGFP-tagged proteins were enriched by immunoprecipitation from soluble lysate of the yeast strains shown in Figure 2G and analyzed by SDS-PAGE and anti-GFP western blotting.

**FIGURE S5 (referring to Figure 3)**
**Comparison of Ski7 and Rrp6 binding to the exosome**
(A) Comparison of Ski7 and Rrp6 binding in patch 1. 5jea and 5c0w are shown side by side. Representation and colors like Figure 3C and Rrp6 in red.
(B) Comparison of Ski7 and Rrp6 binding in patch 2. 5jea and 5c0w are shown side by side. Representation and colors like Figure 3D and Rrp6 in red.
(C) Rrp6 interaction with Rrp43. Representation and colors like Supplemental figure S4B. The Rrp43 residues that were mutated for the pull down in Figure 3D are represented as sticks.

## SUPPLEMENTAL EXPERIMENTAL PROCEDURES

### Purification of yeast exosome subunits

*S. cerevisiae* $Exo_9$, Rrp44 (1-1001, D171N, D551N) and $Rrp6_{exo}$ (518-693) were expressed in *E. coli* and purified with similar protocols as described before (Bonneau et al., 2009; Makino et al., 2013), with the main difference that we used an N-terminally truncated Rrp4 (residues 51-359) and a C-terminally truncated Rrp46 (residues 1-223) to remove regions that were disordered in previous structures. For some of the pull-downs full length Rrp4 was used with the same experimental outcome. Furthermore, it was crucial to employ a lysis buffer containing 1M KCl for high yields of nucleotide-free full length Rrp44. In all expression vectors (except the Rrp43/Rrp46 plasmid) we replaced TEV (tobacco etch virus) cleavage sites with a Prescission protease cleavage site.

### Purification of human exosome subunits and $HBS1L3_{exo}$

*H. sapiens* $Exo_9$ proteins were expressed and purified similarly to the protocols previously described (Greimann and Lima, 2008) with the following exceptions: Rrp42, Mtr3 and Rrp43 were co-expressed and the ternary complex was purified via Ni-affinity chromatography, ion exchange and size exclusion chromatography. For all subunits a high salt wash with 1M NaCl, 50mM KCl, 10mM $MgCl_2$ and 2mM ATP was included in the first Ni-affinity step to remove chaperones and nucleic acids from the sample. Prescission Protease was used to remove $His_{10}$- and SUMO-tags after the initial Ni-affinity step. $HBS1L3_{exo}$ (540-632) was expressed in *E. coli* with N-terminal $His_6$-thioredoxin-tag and C-terminal GFP-tag. The protein was purified on a Ni-affinity column, a reverse Ni-affinity step after cleavage of the thioredoxin-tag with Prescission Protease, followed by size exclusion chromatography.

### Yeast strain generation

Starting from a haploid *ski7Δ* strain, PCR generated mutated *ski7-EGFP::kanMX4* constructs were integrated at the genomic locus by gene replacement. The haploid strains bearing the *ski7* mutations were mated with a *Δxrn1* strain carrying the YCplac33-XRN1 rescue plasmid. The resulting diploid strains were sporulated and tetrads were analyzed to select haploid cells for the desired combination of *Δxrn1* or *XRN1* and *ski7* constructs. Detailed descriptions of the genotypes are listed in Table S1.

### Spotting assays

Cells were grown to an $OD_{600nm}$ of 0.5 in 20 ml of Yeast extract-peptone-dextrose medium supplemented with adenine (YPAD), starting from a saturated overnight culture in SC w/o URA. Except the W303 wildtype strain that was grown in YPAD. 1 $OD_{600nm}$ of cells was harvested and suspended in 200 µl $H_2O$. The cell suspension was serially diluted 1:5 in 96 well plates and then spotted onto the following media plates: YPAD, YPAD-G418 (200 mg/l), YPAD-Nat (100 mg/l), SC w/o URA, SC-FOA (uracil 50 mg/l ; 5-FOA 1gr/l). Cells were grown for 3 days at 30°C. SC: synthetic complete medium; URA: uracil; 5-FOA: 5-fluoroorotic acid.

### Western blot analysis

Cells were grown in 200 ml YPAD to an $OD_{600nm}$ of 3. 200 $OD_{600nm}$ of cells were harvested and suspended in 750 µl of lysis buffer (20 mM Hepes, 150 mM NaCl, 0.5 mM EDTA pH 7.4 supplemented with 1mM PMSF and Roche EDTA free protease inhibitor according to instructions). 0.5 mm glass beads were added to 1/3 of the total volume. Cells were lysed in a Precellys Evolution bead beater at 7500 rpm, 5 cycles of 20 s and 45 s pause. The temperature was kept within -2 °C and 2 °C with the Precellys Cryolys cooling device. Lysates were cleared at 13000 rpm for 15 min at 4 °C in a tabletop centrifuge. 200 µl of the supernatant/lysate was incubated with 25 µl GFP-trap_A slurry (Chromotek) for 2 h at 4 °C on a rotating platform. The agarose beads were spun down at 2000 rpm in a tabletop centrifuge for 5 minutes at 4 °C. The supernatant was removed and the beads were washed twice with lysis/binding buffer. The last wash was transferred to fresh tubes, spun again at 2000 rpm at 4 °C for minutes. The supernatant was removed as much as possible and the agarose beads were immediately resuspended in 2 x SDS loading buffer and boiled for 10 min at 95 °C. 10 µl sample were loaded on a 8-16 % mini-Protean TGX stain free gradient gel (Biorad). The gel was developed and imaged with a Bio-Rad EZ-Imager. Proteins were transferred to a nitrocellulose membrane in 1 x Towbin buffer at 400 mA for 1 h at 4 °C. Immunodetection was done with a Life Technologies iBind device. The primary antibody was an anti-GFP (B-2) monoclonal antibody (Santa Cruz sc-9996) at a concentration of 1:1000 and the secondary antibody was a goat anti mouse HRP conjugated monoclonal antibody (Biorad 172-1011) at a concentration of 1:20000. Detection was done with a GE Healthcare LAS4000 imager.